
INVESTIGATION OF THE EFFECT OF THE ROOF GEOMETRY ON BUILDING THERMAL BEHAVIOUR

Erdal YILDIRIM *
Zeynel Abidin FIRATOĞLU **
Bülent YEŞİLATA **

Received:26.07.2017; revised:27.11.2017; accepted:05.12.2017

Abstract: Main objective of this study is to investigate effect of the roof geometry on indoor air conditions in terms of energy efficiency in summer. Harran's conical roofed building has for this purpose been compared with flat roofed building of equivalent thermo-physical properties, base area and volume. Three dimensional CFD simulations using the low-Reynolds number modeling (LRNM) and standard $k - \epsilon$ turbulence models are performed. The effect of roof geometry on natural ventilation is investigated. Cross ventilation flow rates and convection heat transfer coefficients for these two roof types are evaluated for this purpose. Cross ventilation flow rate for the house with conical roof is found to be 8% higher than that of the flat one. The result of the numerical analysis reveals as well that the conical roof transfers 30% less heat to interior side for a representative summer day, resulting in lower indoor air temperature in the house.

Keywords: Harran house, Roof geometry, Thermal performance, Natural ventilation, Convection heat transfer coefficient

Çatı Geometrisin Bina Isıl Davranışı Üzerindeki Etkisinin İncelenmesi

Öz: Bu çalışmanın amacı yaz ayları için enerji verimliliği açısından, bina çatı geometrisinin iç ortam havasına etkisini araştırmaktır. Bu amaçla Harran konik çatılı yapıları aynı taban alanı, hacim ve termofiziksel özelliklere sahip düz çatılı bina ile karşılaştırılmıştır. Low-Reynolds Number modeling (LRNM) ve $k-\epsilon$ türbülans modeli kullanılarak üç boyutlu CFD simülasyonu gerçekleştirilmiştir. Çatı geometrisinin doğal havalandırmaya etkisi araştırılmıştır. Bu kapsamda çapraz havalandırma debisi ve taşınım ısı transfer katsayıları değerlendirilmiştir. Harran evi çapraz havalandırma açısından düz çatılı yapıya göre % 8 daha iyi performans göstermektedir. Sayısal analizler sonucundan tipik bir yaz günü için Harran evinin kubbesinin düz çatıdan % 30 daha az ısı atağına maruz kaldığı ve bunun daha düşük iç ortam havası sıcaklığına neden olduğu ortaya çıkmıştır.

Anahtar Kelimeler: Harran evi, Çatı geometrisi, Isıl performans, Doğal havalandırma, Taşınım ısı transfer

1. INTRODUCTION

Harran houses are located in Harran district of Şanlıurfa Province in Türkiye, which especially differ in the shape of roof from the modern buildings. Interesting roof forms of Harran House shown in Fig. 1 have construction dates back to 7. BC (Özdeniz, et al., 1998). These vernacular buildings are important structures to understand the history and architectural

* Harran University, Şanlıurfa Technical Sciences Vocational School,63200, Şanlıurfa

** Harran University, Department of Mechanical Engineering, Şanlıurfa

Correspondence author: Erdal Yıldırım (erdaly@harran.edu.tr)

features of the region as well as the change in the adaptation to climatic conditions. For the no air conditioning situation, Harran conical domed houses retain the internal air cooler than the flat roofed buildings in the summer days. The effect of the conical roof shape on building thermal behavior needs to be examined for its adaptation to modern low energy buildings.

Başaran (Basaran, 2011) investigated the thermal performance of Harran Houses and emphasized both of the high thermal capacity of the square base walls and the opening at the top of the dome that facilitates the natural ventilation have contributed providing relatively good indoor thermal conditions. Cardinale, et al., 2013, have recently focused on the analysis of Mediterranean vernacular buildings in the view of energy and indoor comfort without use of air conditioning systems. Results show that the thermal mass of the external walls and roof dampers the large external temperature fluctuations. For the summer season the indoor temperature ranges between 25-28 °C, even with the high outdoor air temperature above 35 °C. Geva, et al., 2014, investigated the thermal comfort based on morphological analyses including cross ventilation in a Synagogue. The results show that the synagogue exhibits high discomfort thermal levels especially in summer, because the design of this synagogue did not consider climate conditions. Faghih and Bahadori 2011, investigated the thermal performance of the domed roofs considering the parameters such like air flow around them, solar radiation, radiation heat transfer with sky and the ground, and openings. Their numerical simulation shows that the thermal performance of the domed roof buildings is better compared to the flat roof one under the same conditions. Laborda, et al., 2015, also investigated the effect of a roof monitor skylight to maximize thermal conditions in a house. Al-Jawadi ve Al-Sudany, 2010, compared the thermal behavior of single domed building and identical flat-roof building by a mathematical technique supported by experimental measurements. The final results arrived at dome-system works to lower temperature by about (2-6) °C on average and aids in reaching thermal balance summertime. Pearlmutter, 1993, also compared the indoor temperatures of the flat roof and vaulted roof experimentally and observed that vaulted roof geometry has greater thermal stability. Nguyen and Reiter, 2014, numerically optimized the design of a low-cost housing to examine the role of thermal comfort criteria. The results show that the optimal design of a natural ventilated house and air-conditioned one has differences, so it is needed to propose an adequate design in the early stage of a project.

The objective of present study is to investigate the effect of the conical roof geometry on indoor air temperature by comparing with flat roofs to ascertain which of these two roof geometries is more energy efficient during summer months



Figure 1:
A photograph showing a particular Harran conical domed house

2. METHOD AND CALCULATIONS

2.1. Heat Transfer Through the Roofs and the Walls

In this study, for the convenience of the calculation of the radiation on the conical geometry, the conical roof was modeled as an octagonal pyramid. Each surface of this octagonal pyramid is assumed to be oriented to north, south, west, east, northeast, northwest, southeast, southwest. For the comparison, it is also assumed that the two building model has same material properties, same thickness, same volume and covering the same base area. And the other assumptions as below,

- Heat transfer through the roof and the walls is assumed one-dimensional; in the absence of any heat generation in the wall, the corner effects are negligible and the wall base is insulated.
- Ambient temperature and the solar radiation are assumed constant for an hourly period.
- Thermal conductivity of the wall material is constant.
- The convection heat transfer coefficient between the outer surface of the building and the ambient air is constant (Section 2.2)
- The convection heat transfer between the indoor air and the inner surface of the building has a value of $h_{in} = 2,5 \text{ W/m}^2\text{°C}$ (Wallentén, 2001).

The general form of the heat transfer equation under given conditions is described below, by taking x-direction normal to the wall surface as shown in Fig. 2.

$$\frac{\partial^2 T}{\partial x^2} = \frac{1}{\alpha} \frac{\partial T}{\partial t} \quad (1)$$

Heat transfer from the outer surfaces of the wall and the roof involves with solar radiation, convection, heat transfer with sky and conduction inside the wall and the roof. The boundary conditions at the left and right boundaries can be expressed as,

$$-k \left. \frac{\partial T}{\partial x} \right|_{x=L} = h_{out} (T_{out} - T_4) + \kappa I + \varepsilon \sigma (T_{sky}^4 - (T_4 + 273)^4) \quad (2)$$

$$-k \left. \frac{\partial T}{\partial x} \right|_{x=0} = h_{in} A (T_{in} - T_0) \quad (3)$$

The initial condition is,

$$T(x, t)|_{t=0} = T_{out} \quad (4)$$

Initial temperatures of the walls, the roof and the indoor air temperature are assumed to be equal to the outside air temperature at 6.00 am. (Fig. 3).

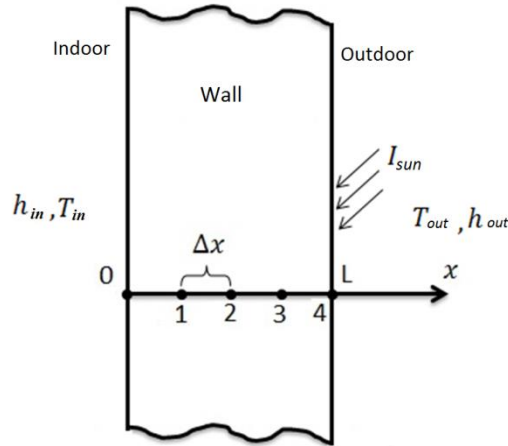


Figure 2:
Configuration of the wall and the roof

With nodal spacing $\Delta x = 0,03 \text{ m}$ the number of nodes M becomes $M = \frac{L}{\Delta x} + 1 = \frac{0,12}{0,03} + 1 = 5$. Thus, there are five unknown nodes of that 1 inner, 1 outer and 3 internal nodes shown with 1, 2, and 3. The equations given below are respectively obtained by applying the energy balance at the left (node 0) and right (node 4) boundaries

$$h_{in}A(T_{in}^i - T_0^i) + kA \frac{T_1^i - T_0^i}{\Delta x} = \rho A \frac{\Delta x}{2} c \frac{T_0^{i+1} - T_0^i}{\Delta t} \quad (5)$$

$$h_{out}A(T_{out}^i - T_4^i) + \kappa AI + \varepsilon \sigma A(T_{out}^4 - (T_4^i + 273)^4) + kA \frac{T_3^i - T_4^i}{\Delta x} = \rho A \frac{\Delta x}{2} c \frac{T_4^{i+1} - T_4^i}{\Delta t} \quad (6)$$

The valid equations for internal planes (nodes of 1, 2, and 3)

$$kA \frac{T_{m-1}^i - T_m^i}{\Delta x} + kA \frac{T_{m+1}^i - T_m^i}{\Delta x} = \rho c A \frac{\Delta x}{2} \frac{T_m^{i+1} - T_m^i}{\Delta t} \quad (7)$$

where κ is the absorptivity, A is the surface area, I is the solar heat flux incident on the surface of the wall and the roof, ε is the emissivity, σ is the Stefan-Boltzmann constant. We denote $\Delta x, T_m^i, k, c,$ and ρ respectively as distance between the nodes, temperature of the node m at time t , thermal conductivities of the wall, specific heat, and, densities of the wall.

Hourly solar radiation on the horizontal surface with its direct, diffuse and the ground reflected components are calculated by using the methods given in Duffie and Beckman, 1991, based on hourly measured global radiation for horizontal surface in Şanlıurfa. Results are presented in Fig. 3. Sky temperature shown in the figure is on the other hand calculated according to the equation of $T_{sky} = 0,0552 (T_{out})^{1,5}$, where T_{out} describes measured hourly ambient temperature. Incoming solar radiation values per unit area of roof are then evaluated for both conical and flat roofs. Each unit area of the flat roof surface receives much higher solar radiation as demonstrated in Fig. 4.

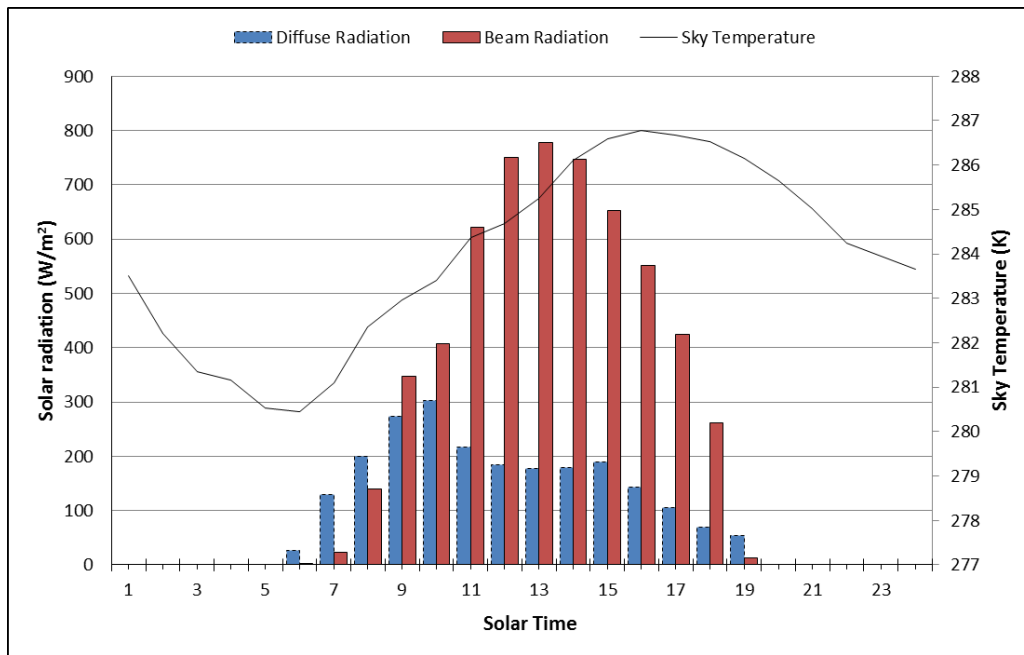


Figure 3:

Components of the horizontal radiation and the sky temperature for a typical summer day

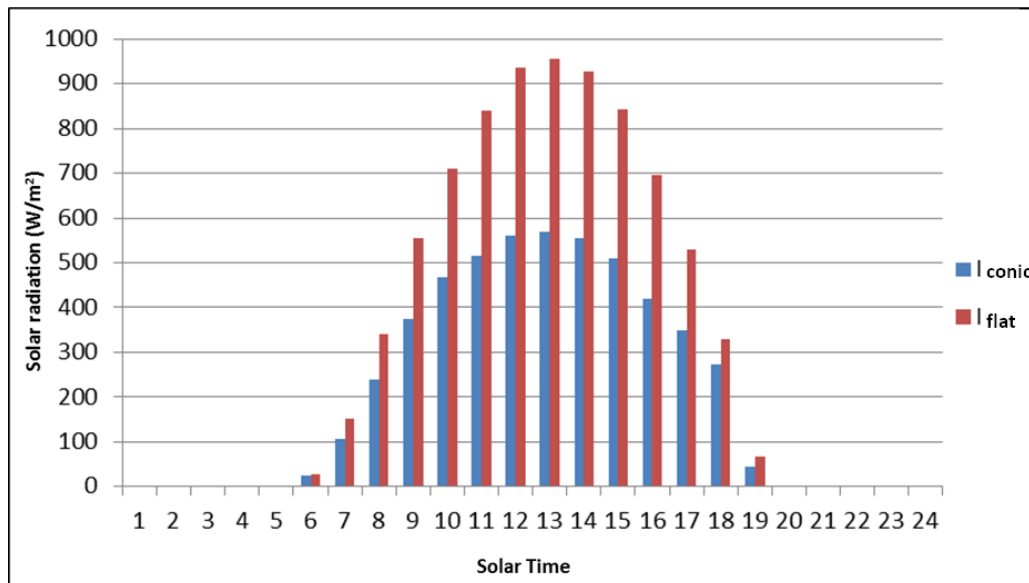


Figure 4:

Solar radiation on the unit area of the conical and the flat roof

The energy balance for the room air, assuming no opening on the building and negligible the radiation exchange between interior surfaces, can be written as,

$$\sum_1^j h_{in} A_i (T_{j,t} - T_{in}^i) + \dot{m}c_p(T_{out} - T_{in}^i) = \rho_a V c_a \frac{T_{in}^{i+1} - T_{in}^i}{\Delta t} \quad (8)$$

where $T_{j,t}$ and T_{in}^i are respectively temperatures of the j th inner surface and interior air at time t , On the other hand, ρ_a is air density, c_a is specific heat of air, and, V is volume of the room.

2.2. Calculation of Convection Heat Transfer Coefficient on the Roof and the Walls of the House

Three dimensional CFD simulation are performed to determine the convective heat transfer coefficient on the roof and the walls of the conical domed and the flat roof houses. Autodesk CFD Simulation 2013 is used for the analysis. The models are employed for an actual sized room of conical domed Harran house, provided that the flat roof building has same volume and same base with its domed counterpart.

The convective heat transfer coefficient is calculated with a fundamental equation given below,

$$h(x) = \frac{q(x)}{T_s(x) - T_a(x)} \quad (9)$$

where $T_a(x) = 293 \text{ K}$ is a constant value specified at that ambient conditions in software and the building surface temperature is accepted as constant, $T_s(x) = 303 \text{ K}$. The dimension of the flat roof building is $3 \text{ m} \times 3 \text{ m} \times 2,9 \text{ m}$, satisfying with the same volume and same base area assumptions, since the base wall dimension of the conical building is $3 \text{ m} \times 3 \text{ m} \times 2,2 \text{ m}$. The Harran house's dome is accepted as a conical dome because its typical dimensions well fit with conical geometry as photographed in Fig. 1. The conical roof height is $2,7 \text{ m}$ and the base radius is $1,5 \text{ m}$. The buildings are located 9 m away from inlet plane. The dimension of the computational domain is $15 \text{ m} \times 15 \text{ m} \times 36 \text{ m}$. Dimensional, wall mesh structure and geometrical features of the computational domain is shown in Fig. 5.

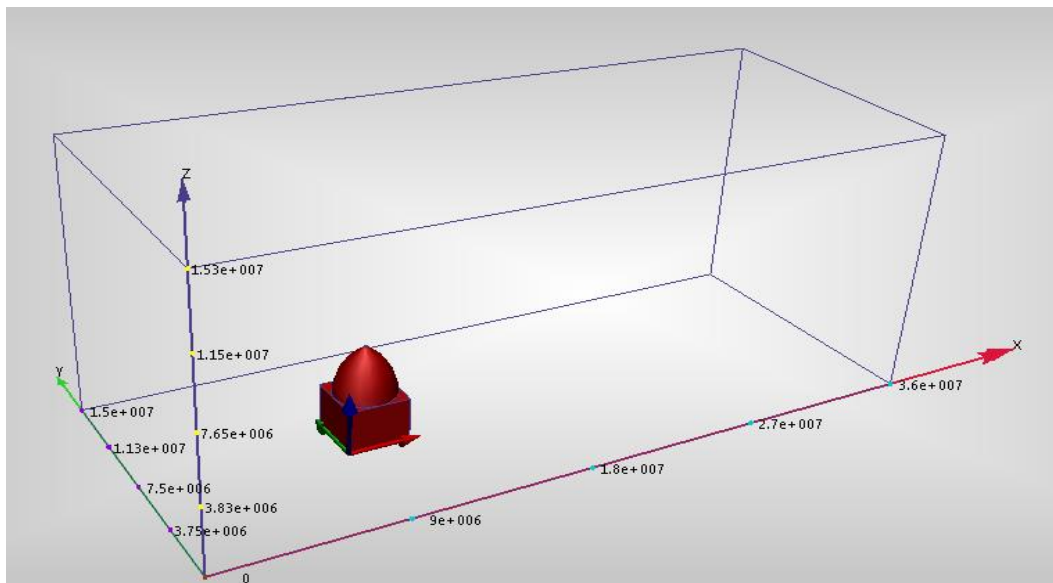


Figure 5:
The dimensions of the computational domain

Tetrahedral mesh type with approximately 1,5 million cells is used in this analysis, under the best allowable memory limit and speed of the computer available in our high performance computer lab. In addition, simulations were made in two different mesh structures and the deviations were found to be below 5%. Hence, the result is that the simulation is independent of mesh structure. The inlet plane wind speed is chosen 2 m/s to simulate average summer wind speed for Şanlıurfa (Şanlıurfa İl Çevre Durum Raporu) and the outlet plane is accepted 0 Pa

static pressure as boundary conditions. The both side planes of the computation domain's boundary condition is accepted as Slip/Symmetry (Blocken et al., 2009; Defraeye et al., 2010) for the computing time saving. The LRNM k-ε model is employed in the simulation due to the fact that the model has been shown to be very convenient with experimental data for such simulations (Blocken et al., 2009; Defraeye et al., 2013).

Considering the studies on the calculation of the coefficient of transport on the surface of the building using various turbulence models (LRNM k-ε turbulence model), CFD simulation results show that the experimental results are compatible with the results of the studies in the literature (Blocken et al., 2009; Defraeye et al., 2010). The CFR simulation results show that the LRNM k-ε turbulence model has proven to be compatible with experimental data. For this reason, the LRNM k-ε turbulence model and the standard k-ε model are used for calculating the convection heat transfer coefficient in the roof of the house of Harran and the flat roof.

2.3. Investigation of Effect of Roof Geometry on Ventilation

This section will compare the conical and flat roofed buildings in natural ventilation flow rates. For this purpose, CFD simulation performed with using $k - \varepsilon$ turbulence model which is effective and widely used in various engineering applications (Nguyen and Reiter, 2014). The domain decomposition technique (Meroney, 2009) is used to predict opening flow rates. Same opening locations added to both building models to find pressure coefficients which are shown in Fig. 6. The boundary conditions are set to the same as CFD analysis in Sec 2.2 except the inlet velocity which is accepted as 5 m/s according to wind profile $V_{inlet} = 0,35 * V_{met} h^{0,25}$ in this case. V_{met} meteorological wind speed was assumed as 10 m/s and h is the height (Allocca, 2003).

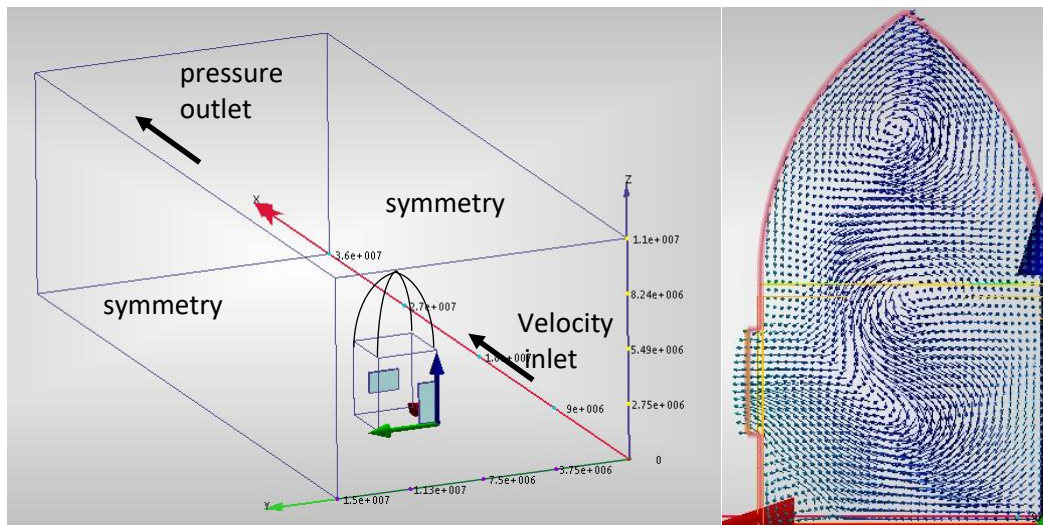


Figure 6:

Computational domain and wind flow pattern inside Harran house

The opening flow rates for the cross ventilation is calculated from the relations below,

$$Q = C_d A U_{ref} \sqrt{C_{p_{in}} - C_{p_{internal}}} \quad (10)$$

$$C_{p_{internal}} = (C_{p_{in}} + C_{p_{out}})/2 \quad (11)$$

where C_d is the discharge coefficient, A is opening area, U_{ref} is approaching wind speed at building height, $C_{p_{in}}$ and $C_{p_{out}}$ are pressure coefficients.

The air flow velocities through the openings on the roof of the Harran house are measured to calculate the energy transferred by the air (Fig.7). The cross section areas of the openings are 15cm by 15 cm. The measurements were performed by Testo 435 anemometer during an hour with 10 minutes periods. The energy transported with air movement from the roof openings can be calculated by adding mass flow rate of air, \dot{m} in Equation (8). This kind of wind velocity roughly causes more than 1000 W energy exchange between inside and outside, and this result is nearly same with Ref (Başaran T., 2011)

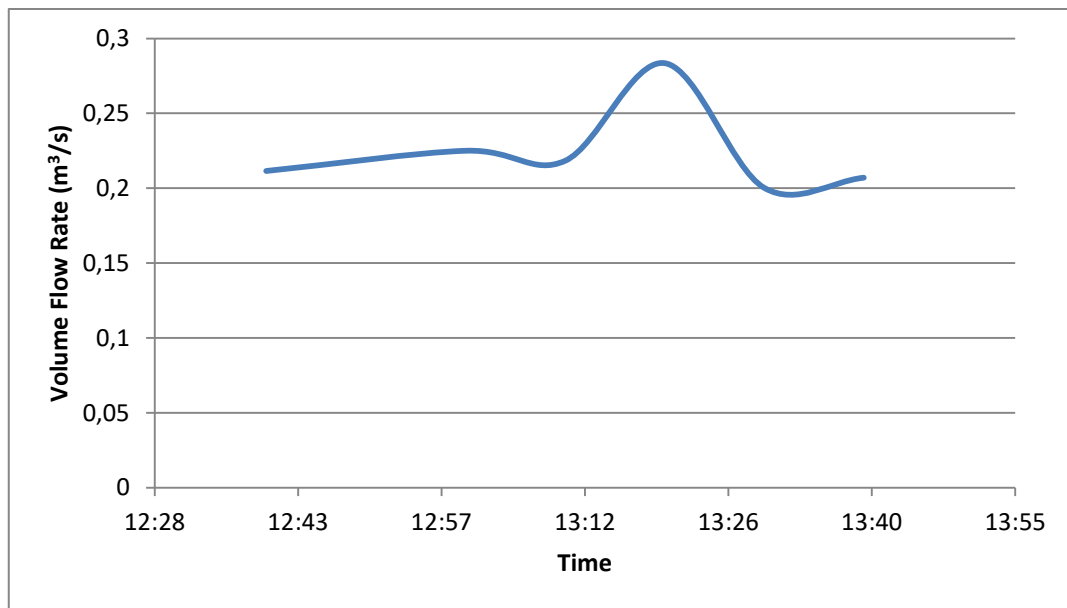


Figure 7:

Average of hourly volumetric flow rate through the openings of the Harran house dome.

3. RESULTS AND DISCUSSION

As a result of the CFD simulation for the scenario which wind blows with 2 m/s speed from west, the distribution of the convection heat transfer coefficients for the building surfaces are determined and shown in Fig. 8. These point-wise values throughout surfaces are averaged and results are summarized in Table 1 for both houses with conical and flat roofs. It is clear from the table that the conical roof house has higher convective heat transfer coefficient on windward side but a lower value on the roof.

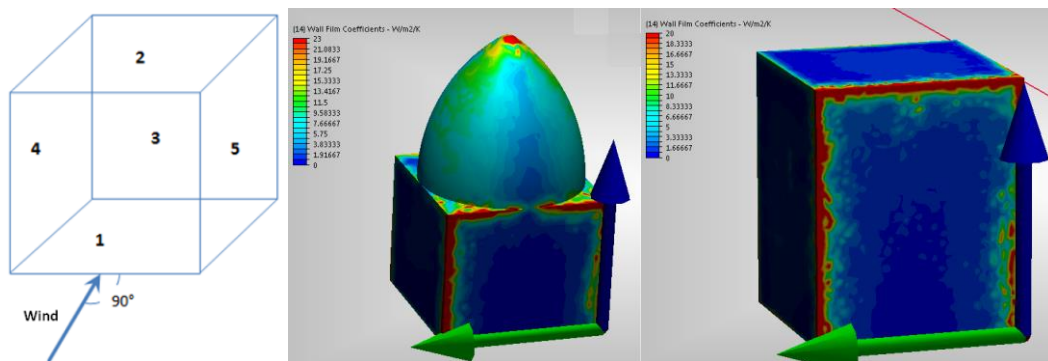


Figure 8:

Distribution of convective heat transfer coefficient along surfaces of the houses

Table 1. The convection heat transfer coefficients for both the flat and the conical roof building surfaces, obtained by CFD simulation.

	Surface	Convection heat transfer coefficient (W/m^2K)	
		Flat roof building	Conical roof building
(1)	Windward	13.54 W/m^2K	18.02 W/m^2K
(2)	Roof	7.95 W/m^2K	5.15 W/m^2K
(3)	Leeward	2.84 W/m^2K	1.81 W/m^2K
(4)	Side	6.72 W/m^2K	8,40 W/m^2K
(5)	Side	6.93 W/m^2K	7.80 W/m^2K

The mean values of volumetric flow rates for two roof models are computed based on CFD analysis outputs. Obtained results are presented in Table 2. The conical roofed house has relatively higher flow rate than the flat one. Percentagewise difference is nearly 8% in favor of the conical roof.

As a result of the analysis, $y^+ < 5$ result plotted for the y^+ value $k-\epsilon$ turbulence model was obtained (Figure 9). As expected, in the standard $k-\epsilon$ turbulence model, the result is 50% higher than the LRNM $k-\epsilon$ turbulence model on the windward side for a flat roofed building. This result is similar to that of Blocken et al., 2009. The results of LRNM $k-\epsilon$ turbulence model were given in this study

Table 2. CFD simulation results and calculations for the ventilation analysis

	Cp_{in}	$Cp_{internal}$	Q (m^3/s)
Conic roofed building	0.9	0.2415	3.795
Flat roofed building	0.912	0.2642	3.528

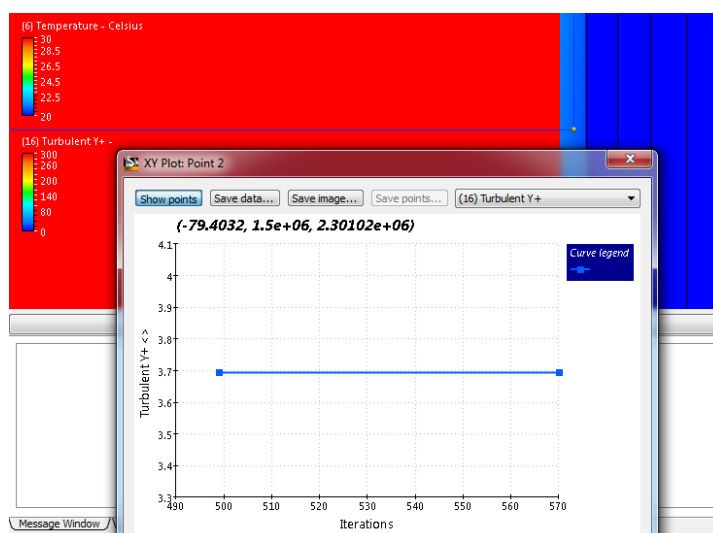


Figure 9:
 y^+ value on the $k-\epsilon$ turbulence model

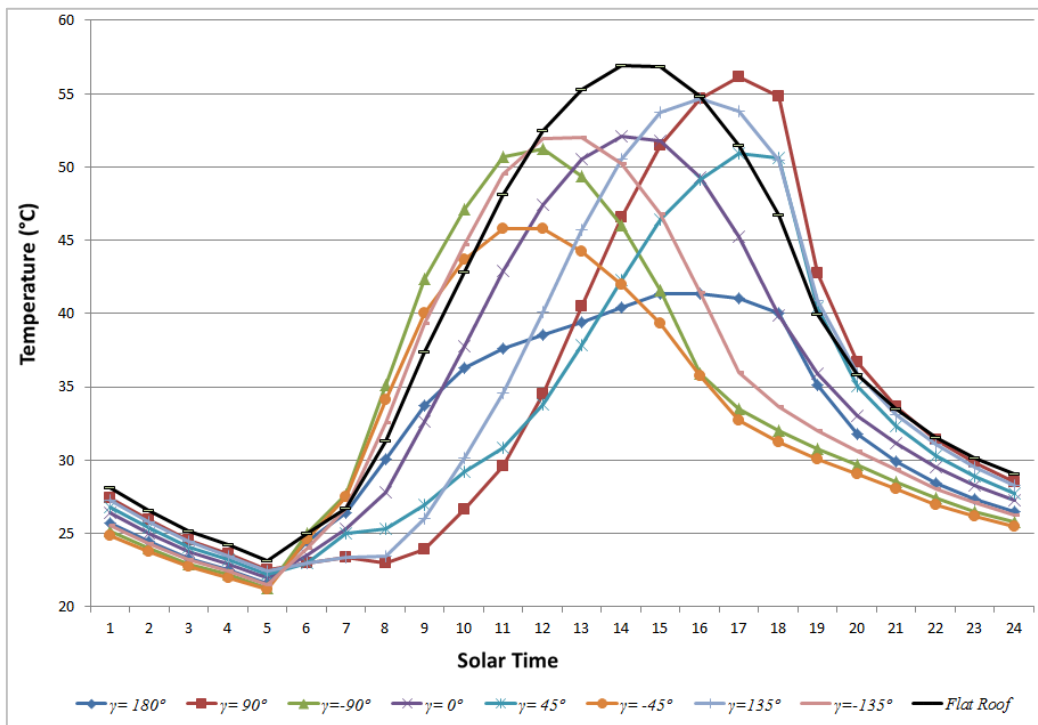


Figure 9:
The variation of the outer surface temperatures at different points of the conical roof with slope ($\beta = 60^\circ$) and the flat roof

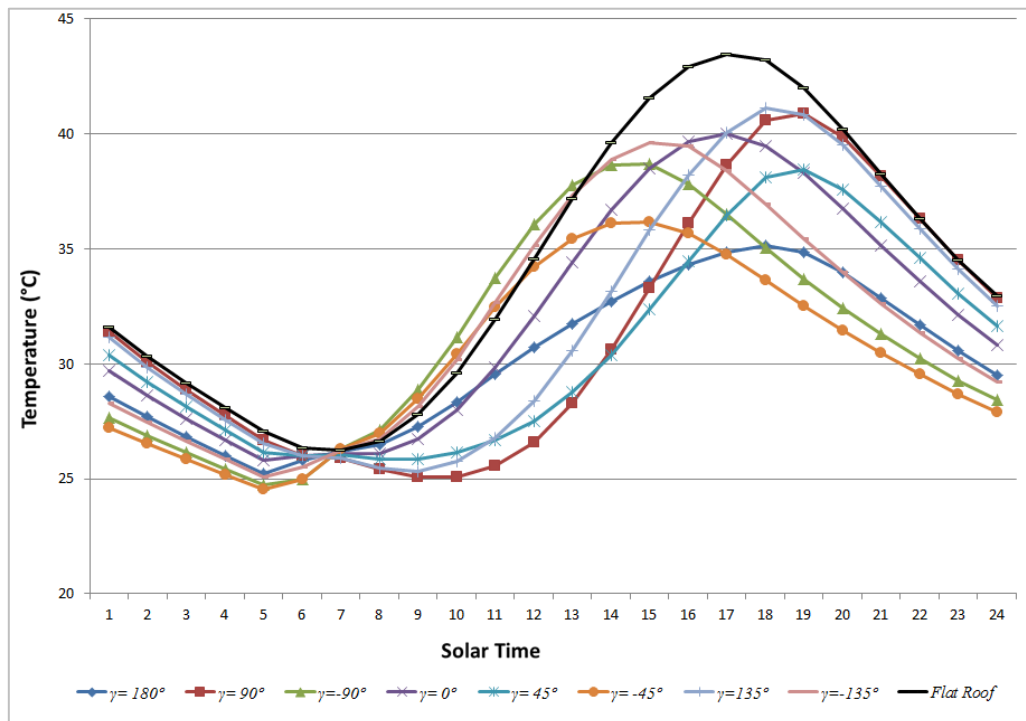


Figure 10:
The variation of the inner surface temperature at different points of the conical roof and the flat roof

Heat transfer analysis of the outer and the inner surface of the walls and the roofs allow calculation of surface temperatures. The average values of hourly outer surface temperatures for both roofs are presented in Fig. 10 for different surface azimuth angles facing in eight directions during the summer day. The outer surface temperatures for the flat roof are always greater than those of the conical roof. The flat roof outer surface temperature is the highest between 11.00 and 16.00. Variation of inner surface temperatures for both roofs are also calculated and shown in Fig. 11. The inner surface temperatures for the flat roof are again higher comparing with the conical roof one. Temperature measurements by a high resolution thermal camera were performed on the inner surface of the conical roof at surface azimuth angle $\gamma=180^\circ$. The image is shown in Fig. 12. The calculated value for corresponding time and surface of the conical roofed house is nearly 32°C and there is well-match with the experimental value obtained from the thermal camera measurements.

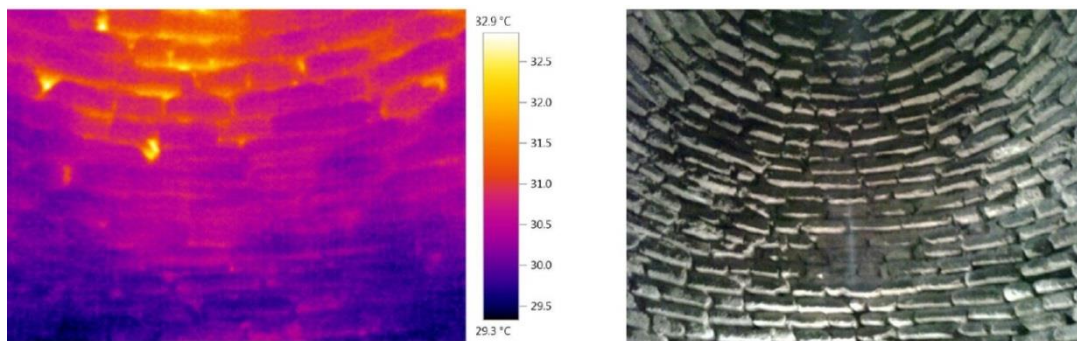


Figure 11:

The infrared image of the node at $\gamma=180^\circ$ on the roof of the conical domed Harran house at 14:00 on 4 June 2013 in Harran.

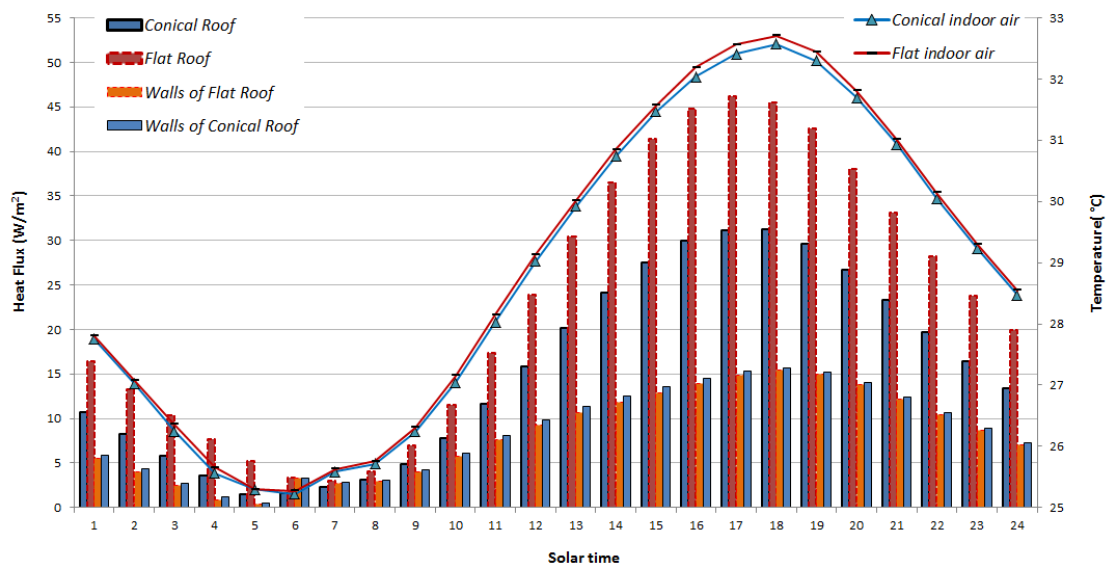


Figure 12:

The comparison of the hourly indoor air temperatures and the total heat flux through the roof and the walls of the Harran house and the flat one

The heat flux through indoor air from roofs and the walls are calculated for comparison and the results are shown in Fig. 13. The heat flux from the flat roof to indoor air is higher and it

reaches the highest value between 17.00-18.00, corresponding to nearly 50% more heat attack to the interior air. On the other hand, Fig. 12 indicates that there is no significant difference between the heat fluxes of both houses through indoor air from the walls.

By using inner surface temperatures of the two building models, the energy balance is applied to the room air, with the assumption of no openings on the buildings. This analysis gives the indoor air temperature fluctuations for a typical summer day (Fig 13). This graph shows that heat flow to conical roof is lower than the flat roof during the day and this is the main cause for the conical roofed house to have better indoor air temperature in summer.

4. CONCLUSION

In this study, the conical and flat roof geometries were investigated in terms of energy efficient roof geometry for summer season. Both of the building models have equivalent thermo-physical properties, same base area and same indoor air volume. The following conclusions summarize the analysis in this study;

- (1) The conical roofed Harran house has lower indoor air temperature than the flat roofed house during a summer day.
- (2) The conical roofed house has an advantage of the less daily total heat transfer to indoor air from walls because of the less surface area. At the end of the typical summer day, the roof of the Harran house is also exposed to $\sim 30\%$ less heat attack ($370,7 W/m^2$) than roof of the flat building ($553,8 W/m^2$).
- (3) At any time of the day, the outer surface temperature of Harran house dome is different with changing surface azimuth angles but the outer surface temperature of flat roof is uniform. This difference for conical roof is $\sim 10^\circ C$ respects to surface azimuth angle, mainly depends on solar radiation incidence In fact this temperature difference helps heat remove from the roof.
- (4) In the case of wind incidence angle of 90° and cross ventilation, the Harran house has better ($\sim 8\%$) performance than flat roofed building.
- (5) In real conditions, Harran houses have one opening on the top and a few on the base of the roof, so these openings causes the vertical ventilation and thus help the heat rejection by the heated air accumulated under the roof, and its value is found $\sim 1000 W$ for Harran house dome.
- (6) The inner surface of the Harran dome has finned form and this situation increases the rate of heat transfer from the inner surface to medium, thus it causes the roof to cool and circulate of air under roof so further research is needed to evaluate this fact.

REFERENCES

1. Al-Jawadi, M. H., Al-Sudany J. A. (2010). Domes and their Impact on Thermal Environment inside Buildings, *World Congress on Housing*, October 26-29, Santander, Spain.
2. Allocca, C., Chen, Q., Glicksman, L. R., (2003) Design analysis of single-sided natural ventilation, *Energy and Buildings*, Volume 35, Issue 8, Pages 785-795, ISSN 0378-7788. [https://doi.org/10.1016/S0378-7788\(02\)00239-6](https://doi.org/10.1016/S0378-7788(02)00239-6)
3. Başaran T. (2011) Thermal Analysis of the Domed Vernacular Houses of Harran, Turkey, *Indoor and Built Environment*, 20(5), 543-554. <https://doi.org/10.1177/1420326X11411237>
4. Blocken, B.J.E., Defraeye, T.W.J., Derome, D. & Carmeliet, J.E. (2009). High-resolution CFD simulations of forced convective heat transfer coefficients at the facade of a low-rise building. *Building and Environment*, 44(12), 2396-2412. <https://doi.org/10.1016/j.buildenv.2009.04.004>

5. Cardinale, N. Rospi, G., Stefanizzi, P.(2013) Energy and microclimatic performance of Mediterranean vernacular buildings: The Sassi district of Matera and the Trulli district of Alberobello, *Building and Environment*, Volume 59, Pages 590-598. <https://doi.org/10.1016/j.buildenv.2012.10.006>
6. Defraeye, T.W.J., Blocken, B.J.E. & Carmeliet, J.E. (2009). CFD analysis of convective heat transfer coefficients on the exterior surfaces of a cubic building. Conference Paper: *Proceedings of the 7th International Conference on Urban Climate*, 29 June – 3 July, Yokohama, Japan, 1-4.
7. Duffie, J.A., Beckman, W.A. (1991). *Solar Engineering Thermal Process*. New York, Wiley Interscience
8. Faghih, A. K. and Bahadori, M. N. (2011) Thermal performance evaluation of domed roofs, *Energy and Buildings*, Volume 43, Issue 6, June 2011, Pages 1254-1263. <https://doi.org/10.1016/j.enbuild.2011.01.002>
9. Geva, A., Saaroni, H. Jacob Morris, J. (2014) Measurements and simulations of thermal comfort: a synagogue in Tel Aviv, Israel, *Journal of Building Performance Simulation*, Vol. 7, Iss. 3. <https://doi.org/10.1080/19401493.2013.819530>
10. Laborda, M. A. C., García, I. A., Escudero, J.F., Sendra, J.J. (2015) Towards finding the optimal location of a ventilation inlet in a roof monitor skylight, using visual and thermal performance criteria, for dwellings in a Mediterranean climate, *Journal of Building Performance Simulation*, Vol. 8, Iss. 4. <https://doi.org/10.1080/19401493.2014.913683>
11. Meroney R. N. (2009) CFD Prediction of Airflow in Buildings for Natural Ventilation, *11th Americas Conference on Wind Engineering*, June 22-26, San Juan, Puerto Rico.
12. Nguyen, A.T., Reiter, S. (2011) The effect of ceiling configurations on indoor air motion and ventilation flow rates, *Building and Environment*, Volume 46, Issue 5, Pages 1211-1222. <https://doi.org/10.1016/j.buildenv.2010.12.016>
13. Nguyen, A.T., Reiter, S. (2014) Passive designs and strategies for low-cost housing using simulation-based optimization and different thermal comfort criteria, *Journal of Building Performance Simulation*, Vol. 7, Iss. 1, 2014. <https://doi.org/10.1080/19401493.2013.770067>
14. Özdeniz, M. B., Bekleyen, A., Gönül, I. A., Gönül, H., Sarigul, H., Ilter, T., Dalkılıç, N., Yildirim, M. (1998) Vernacular Domed Houses of Harran, Turkey, *Habitat International*, vol. 22 issue 4 December, 1998. p. 477-485. [https://doi.org/10.1016/S0197-3975\(98\)00027-7](https://doi.org/10.1016/S0197-3975(98)00027-7)
15. Pearlmutter D. (1993) Roof Geometry as a Determinant of Thermal Behaviour: A Comparative Study of Vaulted and Flat Surfaces in a Hot-Arid Zone, *Architectural Science Review*, 36 (2), Pages 75-86. <https://doi.org/10.1080/00038628.1993.9696740>
16. Şanlıurfa İl Çevre Durum Raporu (2010), T.C. Şanlıurfa Valiliği İl Çevre ve Orman Müdürlüğü, page 13, Şanlıurfa.
17. Wallentén P. (2001) Convective heat transfer coefficients in a full-scale room with and without furniture, *Building and Environment*, 36: 743–751. [https://doi.org/10.1016/S0360-1323\(00\)00070-6](https://doi.org/10.1016/S0360-1323(00)00070-6)

